

THE LANDSCAPE OF COMPLEX NETWORKS

WEINAN E, JIANFENG LU, AND YUAN YAO

ABSTRACT. Topological landscape is introduced for networks with functions defined on the nodes. By extending the notion of gradient flows to the network setting, critical nodes of different indices are defined. This leads to a concise and hierarchical representation of the network. Persistent homology from computational topology is used to design efficient algorithms for performing such analysis. Applications to some examples in social and biological networks are demonstrated, which show that critical nodes carry important information about structures and dynamics of such networks.

Networks have become ubiquitous tools for describing structures that occur in a variety of fields in the past ten or fifteen years, including biology, social sciences, economics and engineering. To study a network, one has to endow it with some mathematical structure. The simplest mathematical structure on a network is the graph structure. This gives rise to notions such as degrees, paths, connectivity, etc. The distinctions between scale-free networks and small-world networks, for example, can be studied by examining this structure, see for example [1, 2, 3, 4]. But one can endow a network with more sophisticated structures, such as geometric structure as in the theory of manifold learning, [5, 6, 7, 8, 9, 10], or topological structure as in the theory of persistent homology [11, 12, 13, 14]. These structures allow us to probe more deeply into the nature of the network.

In this paper, we discuss how one can endow a network with a *landscape* when we study a function on the node set. The concept of landscape has been crucial in physics and chemistry in describing complex systems, such as energy landscape [15]. The introduction of such a concept into complex networks may equip us with a concise description of global structures of networks and help explain certain dynamics such as information diffusion and transition pathways. Many complex networks in real world carry flows of information, products, power, etc., which are driven by local gradients of a scalar or energy [16, 17]. For example traffic flows may be driven by congestion function, heat flows are driven by temperature. In biomolecular folding, conformational changes are driven by the free energy of states. On internet, user's attention may be driven by the centrality or significance of websites such as PageRank. In these cases, communities or groups emerge as metastable sets of gradient-based dynamics or energy basins. Therefore understanding the landscape of such functions will be crucial to disclose associated dynamics in complex networks.

In the core of the landscape lies the notion of critical nodes. In continuous setting this meets the classical Morse theory in the study of manifolds [19], where critical points can be located by vanishing gradients and their indices can be decided by dimensionality of the unstable manifold passing through. However such an approach can not be applied to the graph settings as there is no unambiguous definition of dimensionality in general. Precisely, consider an undirected graph $G = (V, E)$ with

a function defined on the node set $h : V \rightarrow \mathbb{R}$. The question we will attempt to address is: *given a function on its nodes, how can we endow the network with a landscape, so that one can distinguish critical nodes such as the local minima, local maxima, and saddles?*

There are several studies in the literature which may lead to critical nodes for graphs by carrying Morse theory to discrete settings. Nevertheless, none of them gives a satisfied answer to the question. In computational geometry one may embed the graph into a 2D-surface and then apply Morse theory for 2-manifolds [20]. However, such a surface embedding is not natural for general graphs in biological and social networks. Another candidate is discrete Morse theory [21], which studies functions defined on all faces of cell complexes and is therefore hard to use in the graph setting above. A related subject is the extension of the Poincare-Hopf theorem to the graph setting, e.g. in [22].

In this paper we present a purely combinatorial approach which starts from a discrete gradient flow induced by the function on graph nodes. Such an approach does not need a surface embedding, and turns out to be closely related to persistent homology in computational topology [11, 13] and discrete Morse theory [21] without studying functions on high dimensional cells. In particular, given a function (often referred to as an energy function) on a network, we will define a discrete gradient flow associated with that function, as well as minimum energy paths between two disjoint sets of nodes. This allows us to define critical nodes or saddles. Roughly speaking, critical nodes are associated with minimum energy paths between node pairs: index-0 critical nodes are simply local minima; index- k critical nodes are the highest energy transition nodes of minimal energy paths connecting index- $(k - 1)$ critical nodes.

Such a critical node analysis, as we show by examples in social networks and biological networks, leads to a concise representation of networks while preserving some important structural properties. In short, the local minima or maxima together with their attraction basins can be interpreted as communities or groups in networks; saddle points act as transition states between different critical points of lower indices. In particular, in social networks index-1 saddles act as hubs in connecting communities; in biomolecular dynamics, index-1 saddles play roles as intermediate or transition states connecting misfolded and native states. In the latter, such an analysis does not rely on commonly used Markov state model, whence can be applied to much more general data analysis. Moreover, this approach leads to a hierarchical classification of nodes in the network and a global visualization of networks adaptive to the landscape of given energy function.

In algorithmic aspect, critical nodes in this paper can be computed at a polynomial time cost with an algorithm based on computational topology by monitoring topological changes over energy level sets, and in nondegenerate case an almost linear algorithm exists which is scalable for the analysis of large scale networks.

1. LANDSCAPE AND CRITICAL NODES

1.1. Discrete Gradient Flow. Throughout this paper we assume that h is injective (one-to-one). Such functions are generic in the space of real functions on V . One may associate a *gradient flow* of h on the graph G , as a map $D_{h,0} : 2^V \rightarrow 2^V$ which maps a subset of vertices to its immediate neighbors with lower h values. More precisely, given $x \in V$, define the neighbor set of x with lower energy

$\mathcal{N}^-(x) = \{y \in \mathcal{N}(x) : h(y) < h(x)\}$ and

$$(1) \quad D_{h,0}(\{x\}) = \begin{cases} \mathcal{N}^-(x), & \text{if } \mathcal{N}^-(x) \neq \emptyset; \\ \{x\}, & \text{otherwise.} \end{cases}$$

For any $X \subseteq V$, we define

$$(2) \quad D_{h,0}(X) = \bigcup_{x \in X} D_{h,0}(\{x\}).$$

Let $D_{h,0}^2 = D_{h,0} \circ D_{h,0}$, etc. We say that y is *reachable* from x , denoted by $x \succ y$ or $y \prec x$, if $y \in D_{h,0}^k(\{x\})$ for some $k \in \mathbb{N}$, i.e., we can find an energy decreasing path from x to y .

Note that our construction of the gradient flow is related to, but different from the gradient network [16, 17], in which each node is only connected to its neighbor with the lowest energy (i.e. the neighbor in the steepest descent direction). We also remark that the gradient flow can be viewed as a “zero temperature” limit of the stochastic gradient flow introduced in [18] in the study of network communities.

1.2. Local minima. The *local minima* of h are those vertices whose h value is no larger than the values of its neighbors.

$$(3) \quad \mathcal{C}_0 = \{x \mid h(x) \leq h(y), \forall y \in \mathcal{N}(x)\}.$$

In other words, the set of local minima are precisely the maximal vertex set of *fixed points* of the gradient flow $D_{h,0}$.

Given a local minimum $x \in V$, its *attraction basin* is defined to be:

$$(4) \quad \mathcal{A}_0(x) = \{y \mid D_{h,0}^\infty(\{y\}) = \{x\}\}.$$

These are the points that reach the local minimum x but not any other local minima.

Boundary or separatrix consists of those nodes which can reach more than one local minimum following the gradient flow

$$(5) \quad \mathcal{B}_0 = \{x \mid |D_{h,0}^\infty(\{x\})| > 1\}.$$

It is clear by definition that we have the non-overlapping decomposition

$$(6) \quad V = \mathcal{B}_0 \bigcup \bigcup_{x \in \mathcal{C}_0} \mathcal{A}_0(x).$$

1.3. Index-1 critical nodes. Our next task is to classify the nodes in \mathcal{B}_0 . We do so according to their role in the pathways connecting the different local minima. In particular, *index-1 critical nodes (saddles)* are defined as the maxima on *local minimum energy paths* connecting different local minima.

Clearly such a definition relies on the notion of *local minimal energy paths*, which depends on the topology of the path space. Given two local minima, we examine all the paths connecting them. If a path γ_1 can be deformed by the gradient flow to another path γ_2 , we say that γ_1 is *deformable* to γ_2 . The *local minimum energy paths* are paths which cannot be deformed by the gradient flow.

To be more precise, given two points $a, b \in V$, we define a *path* from a to b as $\gamma = (w_0 \cdots w_n)$ such that $w_0 = a$, $w_n = b$, and $w_{i+1} \in \mathcal{N}(w_i)$ for $i = 0, \dots, n-1$. We denote the collection of paths from a to b as $\mathcal{P}_{a,b}$.

We note the following elementary lemma, whose proof is obvious.

Lemma 1. *Let $x \succ y$, we can then find a path $\gamma = (w_0 \cdots w_n)$ from x to y such that $h(w_i) > h(w_{i+1})$ for $i = 0, 1, \dots, n-1$.*

Given two paths $\gamma_1, \gamma_2 \in \mathcal{P}_{a,b}$, we say γ_1 is *deformable to* γ_2 , if there is a map $F : \gamma_1 \rightarrow 2^{\gamma_2}$, such that

- (reaching) every node in γ_1 reaches some nodes in γ_2 , i.e. for any $x \in \gamma_1$, $F(x)$ is not empty and for each $y \in F(x) \subset \gamma_2$, $y \prec x$;
- (onto) every node in γ_2 is reachable from γ_1 , i.e. for any $y \in \gamma_2$, there exists $x \in \gamma_1$, so that $y \in F(x)$, or equivalently,

$$\gamma_2 = \bigcup_{x \in \gamma_1} F(x).$$

Let a, b be two local minima. We call a path $\gamma \in \mathcal{P}_{a,b}$ *local minimum energy path*, if it is not deformable to any other path in $\mathcal{P}_{a,b}$.

We define the energy of a path the maximal energy traversed by the path, i.e. $h(\gamma) = \max_{y \in \gamma} h(y)$. From the definition, if γ_2 is deformable to γ_1 , we have $h(\gamma_2) \geq h(\gamma_1)$, so in terms of energy barrier, γ_1 is a more preferable path than γ_2 .

Given a local minimum energy path, we call the node of maximal energy on the path an *index-1 critical node*. The set of all index-1 critical nodes is denoted by \mathcal{C}_1 . We will also call local minima *index-0 critical nodes*, and hence the notation \mathcal{C}_0 .

The following fact gives a characterization of index-1 critical nodes. The proof can be found in the SI.

Proposition 1 (Classification of index-1 critical nodes). *All local minima in \mathcal{B}_0 are index-1 critical nodes. The other index-1 critical nodes will reach one of the local minima in \mathcal{B}_0 by the gradient flow.*

We call the index-1 critical nodes that are also local minima in \mathcal{B}_0 the nondegenerate index-1 critical nodes, the set of which will be denoted as $\bar{\mathcal{C}}_1$. The other index-1 critical nodes are called degenerate. Not every index-1 critical node is a local minimum in \mathcal{B}_0 , for example in some cluster trees (see Figure 1).

1.4. Higher index critical nodes. The procedure presented above can be extended to define higher index critical nodes.

To define index-2 critical nodes, we consider the subgraph with nodes in \mathcal{B}_0 and edges restricted on this subset, denoted by $G_1 = (V_1 = \mathcal{B}_0, E_1)$. The gradient flow $D_{h,1} : 2^{\mathcal{B}_0} \rightarrow 2^{\mathcal{B}_0}$ on \mathcal{B}_0 is defined similarly as for $D_{h,0}$. We define the attraction basins for $x \in \mathcal{C}_1$ as

$$(7) \quad \mathcal{A}_1(x) := \{y \in \mathcal{B}_0 \mid D_{h,1}^\infty(\{y\}) = \{x\}\}.$$

Note that for any nondegenerate index-1 critical node, the attraction basin is nonempty. While for a degenerate index-1 critical node, the attraction basin is an empty set. This explains the notion “degenerate” for the critical nodes that are not local minima in \mathcal{B}_0 .

We define the boundary set as

$$(8) \quad \mathcal{B}_1 = \{x \in \mathcal{B}_0 \mid |D_{h,1}^\infty(\{x\})| > 1\}.$$

As shown in Proposition 1, all local minima on \mathcal{B}_0 are in \mathcal{C}_1 . Therefore, we have the decomposition

$$(9) \quad \mathcal{B}_0 = \mathcal{B}_1 \bigcup \bigcup_{x \in \mathcal{C}_1} \mathcal{A}_1(x) = \mathcal{B}_1 \bigcup \bigcup_{x \in \bar{\mathcal{C}}_1} \mathcal{A}_1(x).$$

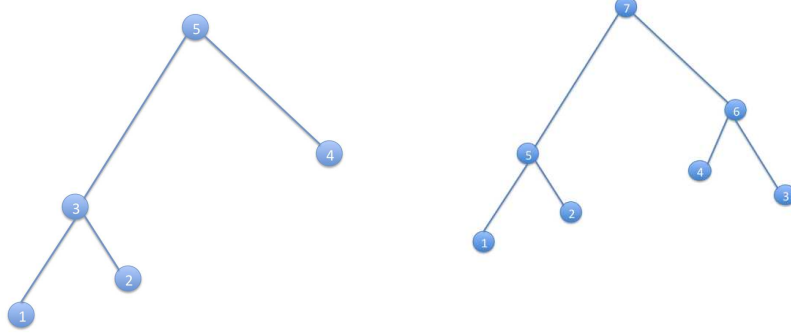


FIGURE 1. Left: an example of degenerate index-1 critical node, where node 5 on top of the tree is a degenerate index-1 saddle while nodes 3 is a nongenerate index-1 saddle. Right: an example of both degenerate and non-degenerate critical node, where node 7 on top of the tree is a degenerate index-1 saddle as it lies on the minimum energy path connecting local minima 1 (or 2) and 3 (or 4), and as well a non-degenerate index-2 saddle as it is on the minimum energy path linking index-1 saddles 5 and 6.

Analogously, we define *index-2 critical nodes* as the maxima on local minimum energy paths connecting different nondegenerate index-1 critical nodes. It is clear that index-2 critical nodes, if exist, must be in \mathcal{B}_1 .

We remark that under our definition, a degenerate index-1 critical node can also be an index-2 critical node, as shown in Figure 1. This ambiguity is actually quite natural from the network point of view, as these points play multiple roles in the structure of the network. The degenerate index-1 critical node can lie either in the basin of a nondegenerate critical node or link together two different nondegenerate critical nodes.

Higher index critical nodes can be defined recursively through further decomposition of \mathcal{B}_1 . Classification for high index critical points can be done following similar arguments as above. Combining these, we obtain:

Theorem 1 (Node Decomposition). *V admits the following decomposition*

$$V = \mathcal{B}_0 \bigcup \bigcup_{x \in \mathcal{C}_0} \mathcal{A}_0(x)$$

where

$$\mathcal{B}_{k-1} = \mathcal{B}_k \bigcup \bigcup_{x \in \mathcal{C}_k} \mathcal{A}_k(x).$$

Here \mathcal{A}_k is the attraction basin of local minima restricted on the $k-1$ -th boundary set \mathcal{B}_{k-1} and \mathcal{C}_k is the set of nondegenerate index- k critical nodes.

The theorem gives us a hierarchical representation of the network associated to the energy landscape. It actually leads to a hypergraph representation whose hypernodes are made up of critical nodes with their attraction basins.

2. FINDING CRITICAL NODES USING PERSISTENT HOMOLOGY

2.1. Persistent homology algorithm.

The landscape introduced above can be naturally formulated in terms of a flooding procedure, from low to high values of the height function $h : V \rightarrow \mathbb{R}$. Flooding starts from local minima, followed by the attraction basins. Once the relevant index-1 saddle is passed, basins of local minima are merged together. This procedure then continues on to critical points of higher indices.

More precisely, this procedure can be described in terms of persistent homology. Persistent homology, firstly proposed by [11] and developed afterwards largely in [12, 13, 14], is an algebraic tool for computing the Betti numbers and homology groups of a simplicial complex when its faces are added sequentially. To work with persistent homology, we extend the graph G into a simplicial complex up to dimension 2, and also define a filtration which consists of such simplicial complexes, in a spirit close to [20] for PL-manifolds.

An abstract simplicial complex Σ_V is a collection of subsets of V , which is closed under deletion or inclusion, i.e. if $\sigma \in \Sigma_V$, then $\tau \in \Sigma_V$ for any $\tau \subset \sigma$.

We define the *flooding complex of network G associated with the function h* , $\Sigma_{G,h} \subseteq 2^V$ as follows:

- 0-simplex: the vertex set V ;
- 1-simplex: the vertex pairs $\{x, y : h(x) \leq h(y)\}$ that $x \prec y$, i.e., $y \in D_{h,0}^k(x)$ for some k ;
- 2-simplex: collections of triangles $\{x, y, z : h(x) \leq h(y) \leq h(z)\}$, such that $x \prec y$ and $y \prec z$.

One can similarly extend the definition above to general k -simplex. However for our purpose it suffices to define up to dimension 2 simplices.

A filtration of flooding complex $\Sigma_{G,h}$ is a nested family $\mathcal{F}_t \subseteq \Sigma_{G,h}$ with $\mathcal{F}_{t-1} \subset \mathcal{F}_t$ which respects the order of deletion or inclusion in $\Sigma_{G,h}$, i.e. if $\sigma \in \mathcal{F}_t$ and $\tau \subset \sigma$ then $\tau \in \mathcal{F}_t$.

Assume that $h : V \rightarrow \mathbb{R}$ is injective or one-to-one, which is generically the case. By taking the maximum over vertices, one can extend h from the vertex set to simplices, and thus to the simplicial complex $\Sigma_{G,h}$. For a simplex $\sigma \in \Sigma_{G,h}$ let $h(\sigma) = \max\{h(i) : i \in \sigma\}$. This implies that a face's h -value is always no more than that of its associated simplex, i.e. $\sigma \subset \tau \Rightarrow h(\sigma) \leq h(\tau)$.

A filtration $(\mathcal{F}_t : t \in \mathbb{N})$ respecting the order of h can be defined in the following way:

- (1) $\mathcal{F}_0 = \emptyset$;
- (2) $\#\{\sigma \in \mathcal{F}_{t+1} \setminus \mathcal{F}_t : \dim(\sigma) = 0\} = 1$, i.e. there is precisely one node being added into the filtration for each step;
- (3) $h(\mathcal{F}_t) < h(\mathcal{F}_{t+1})$, where $h(\mathcal{F}_t) = \max\{h(\sigma) : \sigma \in \mathcal{F}_t\}$, i.e. when a node is added into the filtration, all the simplices of the same energy are added into the filtration simultaneously.

Note that under this construction, \mathcal{F}_1 consists of the global minimum of f .

In this construction, we consider the filtration corresponding to the flooding procedure from low to high h values. The change of Betti numbers identifies the index-0 and index-1 critical nodes. Once the filtration is defined, persistent homology computes the Betti numbers of the simplicial complex in \mathcal{F}_t for each $t \in \mathbb{Z}$,

and draws the barcodes of Betti number versus the t or h values, *e.g.* using JPLEX toolbox¹. The proof of the following theorem is in the SI.

Theorem 2. *Consider the filtration (\mathcal{F}_t) . For all $t \in \mathbb{N}$, $\mathcal{F}_{t+1} \setminus \mathcal{F}_t$ contains an index-0 critical node if and only if β_0 increases from \mathcal{F}_t to \mathcal{F}_{t+1} ; $\mathcal{F}_{t+1} \setminus \mathcal{F}_t$ contains an index-1 critical node if and only if either β_0 decreases or β_1 increases from \mathcal{F}_t to \mathcal{F}_{t+1} .*

To find higher index saddles, we restrict on the subgraph $G_k = (V_k, E_k)$ where $V_k = \mathcal{B}_{k-1} = V \setminus \bigcup_{0 \leq i \leq k-1} \bigcup_{x \in \mathcal{C}_i} \mathcal{A}_i(x)$ and E_k consists of edges restricted on V_k . We can analogously construct the filtration corresponds to the flooding procedure $(\mathcal{F}_{k,t}, t \in \mathbb{N})$ on the subgraph G_k . Similar identification holds for higher index saddles.

Theorem 3. *Consider the filtration $(\mathcal{F}_{k,t})$ on subgraph G_k for $k \geq 2$. For all $t \in \mathbb{N}$ such that $\mathcal{F}_{k,t+1} \setminus \mathcal{F}_{k,t}$ contains an index- k critical node if either β_0 decreases or β_1 increases from $\mathcal{F}_{k,t}$ to $\mathcal{F}_{k,t+1}$.*

Clearly our characterization of high order critical nodes above only exploits simplicial complex up to dimension 2, whose persistent homology computation is recently improved to be of complexity $O(m^{2.376})$ [24] with $m = O(n^3)$ the total number of simplices and n the number of nodes. Such a complexity does not suffer the curse of dimensionality as the computation of high order Betti numbers in general.

2.2. Efficient Search of Nondegenerate Saddles.

As we know from Proposition 1 that nondegenerate critical nodes are actually local minimum in sub-graphs G_k , this leads to an efficient algorithm for finding nondegenerate critical nodes. In fact, all the examples shown in this paper have only nondegenerate critical nodes and thus can be found efficiently using this algorithm.

Given an injective function h on the vertices, we obtain the local minima and nondegenerate index- k saddles using Algorithm 1.

The bottleneck in this algorithm is in finding the attraction basins of local minima, whose complexity can be $O(nd)$ where n is the number of vertices and d is the maximum degree a node has. The total complexity is $O(Knd)$ where K is the maximum index of critical points. The algorithm is much faster than the previous algorithm for finding all critical nodes.

¹<http://comptop.stanford.edu/programs/>

Algorithm 1 Fast search of nondegenerate critical nodes

```

Sort the nodes according to  $h$  in increasing order;
Set  $G_0 = G$ ;
for  $k = 0, \dots, n$  do
  for  $x \in V_k$  in an increasing order of  $h$  do
    Find neighbors of  $x$  with lower energy,  $\mathcal{N}_k^-(x) = \{y \in \mathcal{N}(x) \cap V_k \mid h(y) < h(x)\}$ ;
    if  $\mathcal{N}_k^-(x) = \emptyset$  then
      Add  $x$  to  $\bar{\mathcal{C}}_k$  and set the color of  $x$  as its node index;
    else
      if  $\mathcal{N}_k^-(x)$  contains a single color then
        Set the color of  $x$  as the single color;
      else
        Leave the color of  $x$  as blank;
      end if
    end if
  end for
return :
  (1) local minima  $\bar{\mathcal{C}}_k$  as nondegenerate critical nodes;
  (2) attraction basins  $\mathcal{A}_k(x_0)$  ( $x_0 \in \bar{\mathcal{C}}_k$ ) as color components;
  (3) boundary  $\mathcal{B}_k$  as the blank nodes;
  Set  $G_{k+1} = (\mathcal{B}_k, E_{k+1})$  where  $E_{k+1}$  are edges restricted on  $\mathcal{B}_k$ ;
end for

```

3. EXAMPLES

3.1. Zachary's Karate Club Network. Zachary's karate club network [23] consists of 34 nodes, representing 34 members in a karate club with node 1 being the instructor and node 34 being the president (Figure 2). An edge between two nodes means that the two members join some common activities beyond the normal club classes and meetings. Conflicts broke out between the instructor and the president when the instructor sought to raise the fee and the president opposed the proposal. The club eventually split into two, one formed by the president (blue nodes in Figure 2(a)) and another one led by the instructor (red nodes in Figure 2(a)). A lot of information about this fission can be disclosed by looking at the graph structure of this social network.

Let d_i be the degree of node i , and define $\bar{h}_i = -\log d_i$. To avoid the same degree between two nodes in neighbor, a small enough random perturbation is added such that $h_i = \bar{h}_i + \epsilon_i$ is injective. Figure 2(b) shows the gradient flow of h . The arrows on the edges point from low degree nodes to high degree ones. Note that nodes 24 and 25 both have degree 3, hence a small random perturbation is added resulting in the arrow from 25 to 26. The same is done for nodes 5 and 11.

Figure 2(c) shows the node decomposition for Karate club network with each color component for a critical node and its attraction basin. Two local minima, nodes 1 and 34, are in oval shape together with their attraction basins marked in red and blue, respectively. Two index-1 saddles, nodes 3 and 32, are yellow and green diamond nodes, whose basins are in yellow (nodes 3) and green (node 32) correspondingly. Node 3 is the lowest energy node connecting the local minima nodes 1 and 34 via a minimum energy path $\gamma_1 = (1, 3, 33, 34)$. Node 32 links the two local minima by another local minimum energy path, $\gamma_2 = (1, 32, 34)$. Two index-2 saddles, nodes 25 (in light blue diamond) and 29 (in cyan diamond), which connect

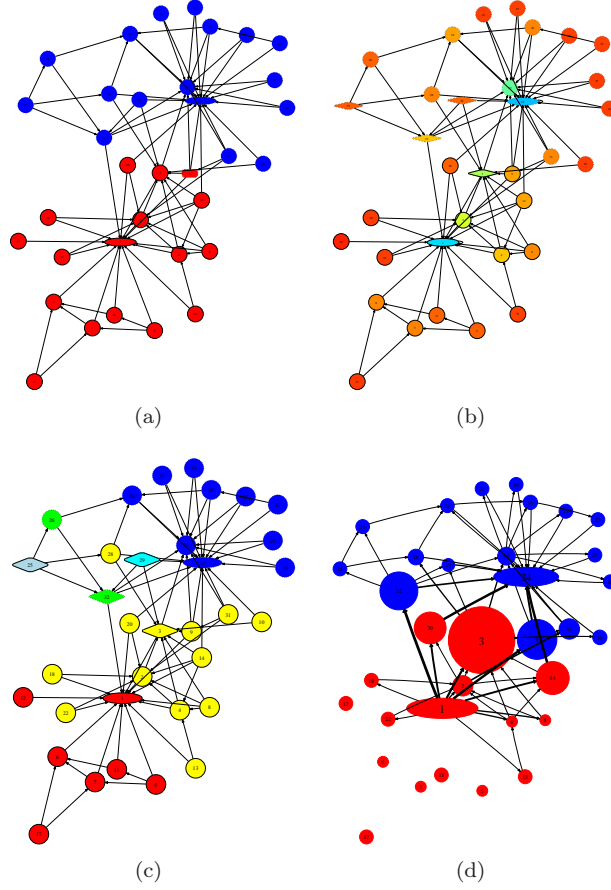


FIGURE 2. Landscape of Karate Club. (a) The fission of Karate Club into two new clubs [23], the coach is node 1 and the president is node 34, where the box node joined the red club (coach) instead of the blue due to his necessity to finish the course. (b) A gradient flow on edges, node colors from blue to red indicate the energy from low to high, four nodes in diamond shape to-be-disclosed soon as critical nodes. (c) Node decomposition with each color component representing a critical node with its basin: two local minima are in oval shape in which node 1 has basin in red and node 34 in blue; two index-1 saddles are in diamond shape in which node 3 has basin in yellow and node 32 in green; two index-2 saddles, node 25 in light blue and node 29 in cyan. (d) A transition path analysis (SI) with source node 1 and target node 34. Committor function with thresholding probability 0.5 is used to divide all the nodes into two communities, one with node 1 in red and the other with node 34 in blue. Node size is in proportion to transition current connecting two communities through the node. Effective reactive currents from node 1 to node 34 are drawn with arrows on edges, whose width is determined from effective reactive current with a threshold greater than 0.001. It can be seen that index-1 saddles (3, 32) host a majority of transition currents.

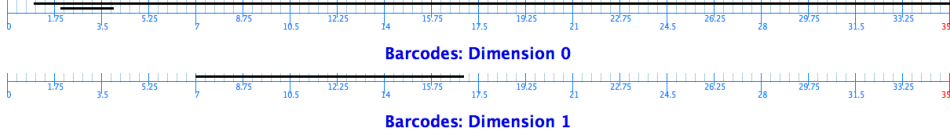


FIGURE 3. Barcodes of Betti numbers for the filtration of Karate Club network. Top: β_0 versus t . Node 34 with the lowest energy is added at $t = 1$ which creates a connected component which never disappears. Node 1 with the second smallest energy is added at $t = 2$ which creates a new connected component disappeared when index-1 saddle 3 is added at $t = 4$. Bottom: β_1 versus t . The loop is created by index-1 saddle 32 added at $t = 7$ then cancelled by index-2 saddle 29 at $t = 17$.

two index-1 saddles via two non-deformable minimal energy paths $(3, 29, 32)$ and $(3, 28, 25, 32)$. Figure 2(d) further depicts a transition path analysis of a Markov chain induced on the graph (see SI) from local minimum node 1 to node 34, which shows two index-1 saddles capture most of transition currents.

Figure 3 shows the barcodes for the flooding complex of this network.

3.2. The social network of Les Misérables. The social network of Les Misérables, collected by Knuth [25], consists of 77 main characters in the novel by Victor Hugo. The edge weight w_{ij} record the number of co-occurrence of two characters i and j in the same scene. Thus it is a weighted graph where $h_i = -\log \sum_{j \sim i} w_{ij}$ as the negative logarithmic weighted degree. The original network exhibits a single local (global) minimum, Valjean, who is the central character as the whole novel was written around his experience.

However, dropping those edges whose weights are no more than a threshold value (7 here), there appears a subnetwork which is closely associated with the Paris uprising on the 5th and 6th of June 1832, see Figure S-1. The subnetwork consists of two local minima, Enjolras and Valjean, the former being the leader of the revolutionary students called *Friends of the ABC*, the Abaissé. Led by Enjolras, its other principal members are Courfeyrac, Combeferre, and Laigle (nicknamed Bossuet) et al., who fought and died in the insurrection. Among them is an index-1 saddle, Courfeyrac, a law student and often seen as the heart of the group, who introduced Marius to the Friends of ABC. Marius, a descend of the Gillenormands, though badly injured in the battle, was saved by the main character Valjean when the barricade fell and married to Cosette, the adopted daughter of Valjean. The landscape of this subnetwork highlights these events in the novel.

3.3. LAO Protein Binding Transition Network. This application examines the binding of Lysine-, Arginine-, Ornithine-binding (LAO) protein to its ligand, recently studied in [26]. The critical node analysis provides us a concise summary of global structure of networks while preserving important pathways, which enables us to reach a more thorough description than previous approximate analysis.

In [26] a Markov state model was constructed with 54 metastable states, using data obtained from molecular dynamics simulation. More information about these states can be found in SI and [26]. Now we examine the transition network as a weighted directed graph $G = (V, E, W)$, where V consists of 54 nodes, each

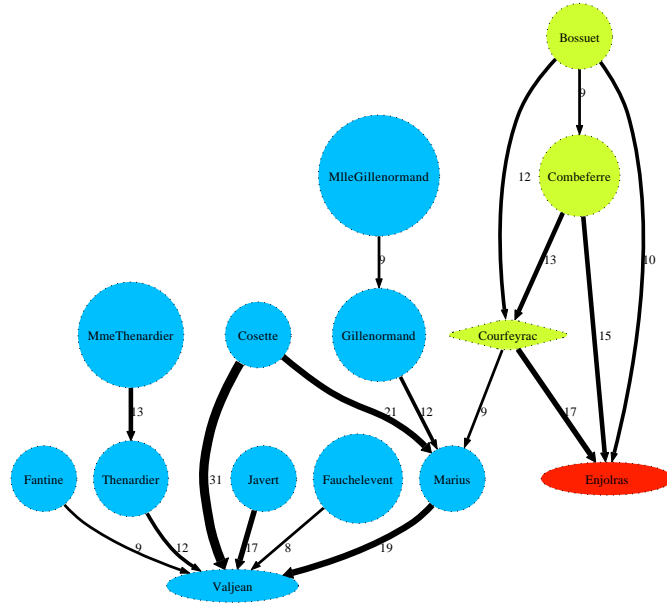


FIGURE 4. Landscape of a subnet of The Les Misérables Network. Edges are left with weights larger than 7. Two local minima, Valjean and Enjolras as well as an index-1 saddle, Courfeyrac, are identified.

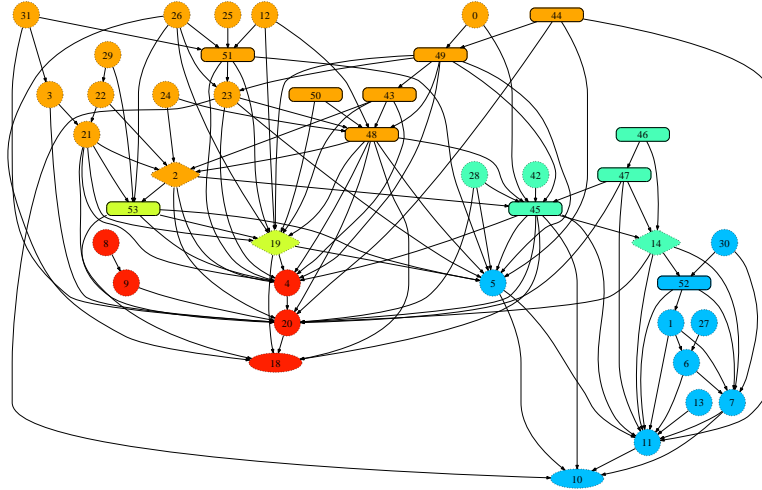


FIGURE 5. Landscape of LAO protein binding. Local minima are represented as ovals, index-1 and index-2 saddles are shown in diamonds, circular nodes are regular nodes, and rectangular nodes are solvated states $\{43, 44, \dots, 53\}$. Color components represent the node decomposition.

representing a metastable state, an edge $(i, j) \in E$ if transitions from node i to j are observed in simulations with 6 ns delays (the implied time scale for approximate Markovian behavior), and the number of transitions is recorded as the weight w_{ij} . Eleven of the states ($\{43, 44, \dots, 54\}$) are solvated or unbound states. The binding state is node 10.

Let $p_{ij} = w_{ij} / \sum_j w_{ij}$ be the transition probability from state i to state j . This defines a Markov chain with a unique stationary distribution π . We threshold this graph to an undirected graph by keeping those edges $\{i, j\}$ such that $\frac{w_{ij} + w_{ji}}{2} > 30$, *i.e.* average count number is larger than 30. One reason for doing this is that small numbers of transitions may be heavily influenced by the noise caused by the way of counting the transition. Note that the mean transition count is about 120, and the qualitative behavior reported below shows certain stability under the variation of the threshold value.

The energy function is $h(i) = -\log \pi(i)$ where π is the stationary distribution of metastable states. Application of the method above gives rise to a landscape shown in Figure 5. Isolated states are dropped in this picture. Colors in this picture illustrate the node decomposition according to Theorem 1, where each color component represents the attraction basin of a critical node. Below we shall discuss structural properties of these nodes. A complete picture of structural information for all 54 states can be found in SI.

There are two major local minima in the landscape, nodes 10 and 18. Node 10 is the bound state which is the minimum in the most populated energy basin. Its attraction basin is colored in light blue. Nodes 11 (population 13.5%) and 5 (population 1.15%) are two encounter complexes in that basin. In these states, the ligand is in or close to the binding site and conformations in this state have a small twist but large opening angles. The other local minimum is node 18, a misbound state, where the ligand interacts with the protein outside the binding site and close to the hinge region of two domains of the protein. State 18, together with state 4, 8, 9, and 20, forms a misbound basin marked in red. In these states, the ligand interacts with the protein from a distance to the binding site. State 8 and 9 exhibit similar structural properties with a negative twisting angle and a fixed distance to the binding site (about 10), while state 4, 18, and 20 exhibit similar but a different type of structures.

Node 19 and 14 are two index-1 saddles connecting the two basins associated with local minima. They are metastable intermediate states between misbound and bound states. But in these saddles ligand interacts with the protein in different ways. In state 19 (population 32%), the ligand is interacting with the protein from one twisting direction (positive) and the protein is quite closed. In a contrast, in state 14 (population 35%) the ligand is approaching the protein from the opposite twisting direction (negative) and the protein is still quite open (see SI). These two saddles actually play different roles in reactive pathways which will be discussed below. Node 2 is an index-2 saddle, which is essentially a high energy misbound state. Note that high index saddles are unstable with respect to different thresholding values. In the following we shall focus on index-1 saddles.

For a quantitative analysis on the roles of index-1 saddles, we conduct two kinds of transition path analysis using transition path theory ([27] or see SI). First, we study reactive currents from the misbound state 18 to the bound state 10. This analysis shows that a majority of flux passes through the saddle 19. Therefore once

the ligand and protein fall in the misbound state 18, the major pathway to escape and enter the bound state is via saddle 19.

The other analysis, as was also did in [26], studies transition paths from the eleven solvated states marked from 43 to 53 to the bound state 10. In particular, we investigate reactive currents from each of the solvated states to the bounded state, respectively. The results are summarized as follows. A large part of these details has been ignored in [26], since they only examined 10 transition pathways, ignoring the others.

- (1) Solvated state 52 lies in the basin of bound state 10, whence misbound state 18 has little influence on its pathway.
- (2) Solvated state 53 only passes through index-1 critical node 19 to enter the bound state 10, which is heavily influenced by the misbound state 18.
- (3) Solvated states $\{45, 46, 47\}$ lie in the basin of index-1 critical node 14 and enter the bound state 10 directly or via 14. They are not much influenced by the misbound state 18.
- (4) Other solvated states are in the basin of index-2 critical node 2. Transition path analysis further shows that misbound state 18 has a stronger influence on them than those in the basin of 14. In particular state 50 is mostly influenced with near 50% of transition currents trapped by the misbound state 18.

In summary, the misbound state 18 affects some of the pathways from solvated states to the bound state. Index-1 critical node 14 is a state where ligand starts to interact with protein to enter the encounter complex 11. If we can design some mutations to disrupt the stability of this state or even encounter complexes, we may be able to make the binding much more difficult. Finally we note that the critical node analysis here does not rely on the Markov model assumption and can thus be applied to the analysis of transition networks in molecular dynamics beyond its Markovian time scale.

4. DISCUSSION AND CONCLUSION

We have introduced a notion of critical points for network which can be used to reduce a complex network to a coarse-grained representation while preserving structural properties associated with functional gradient flows. Examples have shown that the information obtained this way is of great value in capturing global structure and dynamics of the network, such as diffusive or reactive pathways. Moreover, the critical point analysis leads to a hierarchical decomposition which may enable us to perform multiscale analysis of complex networks. These perspectives will be systematically pursued in the future.

An interesting question is the stability of these objects against noise. To answer this question, one has to clarify the source of noise. There are two types of noise one should consider in landscape analysis of networks – one associated with the energy function h and the other associated with the network structure. The former can be dealt with traditional persistent homology denoising, where critical nodes with shallow basins can be merged with their saddles. The latter is however more challenging as there are no systematic studies yet on perturbation or bootstrapping of networks. In the examples above, we used edge thresholding on the Les Misérables and the protein binding networks, which is equivalent to modeling such networks as a superposition of a signal graph and some Erdős-Rényi type random graphs

as noise. However there might be better models which lead to different denoising rules.

ACKNOWLEDGEMENTS

W.E. acknowledges supports from ARO grant W911NF-07-1-0637 and ONR grant N00014-01-1-0674. J.L. is grateful to Eric Vanden-Eijnden for helpful discussions. Y.Y. thanks Xuhui Huang for providing Figure S-2 in supporting information with helpful discussions, as well as supports from the National Basic Research Program of China (973 Program 2011CB809105), NSFC (61071157), Microsoft Research Asia, and a professorship in the Hundred Talents Program at Peking University.

SUPPLEMENTARY INFORMATION

S-1. PROOFS

Proof of Proposition 1. We show first that every local minimum in \mathcal{B}_0 must be an index-1 critical node. Let x be a local minimum in \mathcal{B}_0 . Then x reaches at least two local minima, say $y_1, y_2 \in \mathcal{C}_0$. Consider the subgraph with node set

$$S = (\{x\} \cup \mathcal{A}(y_1) \cup \mathcal{A}(y_2)) \cap \{y \mid h(y) \leq h(x)\}.$$

Clearly, S is connected and x is the unique maximum node in S . By the definition of the attraction basin, the set $S \setminus \{x\}$ is not connected.

Since S is connected, it contains at least a path from y_1 to y_2 . Let γ be the local minimal energy path from y_1 to y_2 in the subgraph S . As $S \setminus \{x\}$ is not connected, γ must pass x , so that $h(\gamma) = h(x)$.

We now show by contradiction that γ is also a local minimal energy path in the original graph V . Suppose we can find another path from y_1 to y_2 , called $\tilde{\gamma}$, so that γ is deformable to $\tilde{\gamma}$. For any $z \in \tilde{\gamma}$, we have $h(z) \leq h(x)$. Consider the set $\tilde{\gamma} \cap \mathcal{B}_0$, which is non-empty. We distinguish two cases:

- a) $\tilde{\gamma} \cap \mathcal{B}_0 = \{x\}$. Then, $\tilde{\gamma} \setminus \{x\} \subset \mathcal{A}(y_1) \cup \mathcal{A}(y_2)$, so that $\tilde{\gamma} \subset S$. By construction of γ , we have $\tilde{\gamma} = \gamma$;
- b) If there exists $z \in \tilde{\gamma} \cap \mathcal{B}_0$ and $z \neq x$, we have some point $x' \in \gamma$ that $z \prec x'$. It is easy to see that x' must be x , since other points on γ are in attraction basins of y_1 and y_2 . Using Lemma 1, there exists a path $\gamma_1 = (w_0 \cdots w_n)$ from z to x ordered in energy increase. In particular, consider the point w_{n-1} , we have $z \prec w_{n-1}$ so that $w_{n-1} \in \mathcal{B}_0$. Moreover, $w_{n-1} \in \mathcal{N}(x)$ and $h(w_{n-1}) < h(x)$. This contradicts with the fact that x is a local minimizer in \mathcal{B}_0 .

Therefore, γ is a local minimal energy path, and x is an index-1 critical node.

Let $z \in \mathcal{C}_1$ which is not a local minimum in \mathcal{B}_0 . Then, z must reach a local minimum x in \mathcal{B}_0 by the gradient flow. By the first part of the proposition, $x \in \mathcal{C}_1$. The proposition is proved. \square

Proof of Theorem 2. (Necessity). We first show that index-0 and index-1 critical nodes, when added into the filtration, will change Betti numbers in the way above.

For index-0 critical nodes, they are local minima of graph G . When a local minima is added into the filtration, it must create a new connected component which increases the 0-th Betti number, β_0 .

Index-1 saddles will play a more complicated role. We have two situations

- if an index-1 saddle lies on top of a global minimal energy path, it will decrease β_0 upon being added;
- if an index-1 saddle lies on top of a local minimal energy path other than the global one, it will increase β_1 upon being added.

Given a pair of index-0 critical nodes $y_1, y_2 \in \mathcal{C}_0$, among all local minimal energy paths connecting them (if exist), there must be a global minimal energy path γ_0 , so that $h(\gamma_0)$ is less than any other local minimal energy paths between y_1 and y_2 . We denote the maximal node of the global minimal energy path as x . Such x is an index-1 critical node. When x is added into the filtration, the 0-th Betti number β_0 will decrease as x connects two components contains y_1 and y_2 respectively.

For the other local minimal energy paths connecting y_1 and y_2 , the associated index-1 critical nodes will increase the first Betti number β_1 when added into the filtration. Indeed, let z be such an index-1 critical node. Thus z is a maximum of a local minimum energy path γ_1 such that $h(\gamma_1) = h(z) > h(x) = h(\gamma_0)$. γ_1 is not deformable to the global minimal energy path γ_0 between y_1 and y_2 . Then two paths γ_0 and γ_1 forms a loop, and hence the first Betti number β_1 increases when z is added into the filtration.

(Sufficiency). We show next that no other nodes when added into the filtration will change the first two Betti numbers in the same way.

For any node x which lies in the attraction basin of a local minima $\mathcal{A}_0(x_0)$ for some $x_0 \neq x$, x reaches x_0 by gradient flow. For any edge $\{x, x'\} \in E$ with $x' \in \mathcal{A}_0(x_0)$, x' reaches x_0 and thus the triangle $\{x, x', x_0\}$ is included in the simplicial complex. This implies that $\mathcal{A}_0(x_0)$ is contractible (star-shape), whence no node in $\mathcal{A}_0(x_0)$ other than local minimum x_0 will change Betti numbers.

It remains to show that any node in boundary $\mathcal{B}_0 \setminus \mathcal{C}_1$ will not change Betti numbers in the same way. Any such node $z \in \mathcal{B}_0$ must reach at least two local minima, say a and b . Then by Lemma 1 there is a path $\gamma = (a = w_0, \dots, z = w_k, \dots, b = w_l)$ for some $l \in \mathbb{N}$ such that $h(w_s) < h(w_{s+1})$ for $s \leq k-1$ and $h(w_s) > h(w_{s+1})$ for $s > k$. Moreover $z \notin \mathcal{C}_1$ implies that γ is deformable to a local minimal energy path $\pi = (a = v_0, \dots, b = v_m)$ between the same end nodes, for some $m \in \mathbb{N}$. z can not decrease number of connected components as the path π , which appears first in the filtration, already connects a and b .

Now we show that the path γ will not create a loop either. Let $\pi_t = c \in \mathcal{C}_1$ be the maximal node on π . We must have $c \prec z$. To see this, as γ is deformable to π , there is a node $c' = w_{k'} \in \gamma$ which reaches $c \in \pi$. We may assume $c' \neq z$ ($k' \neq k$) since otherwise we are done. Then, by the construction of the path γ , we have $c' \prec z$, and hence $c \prec z$.

Note that both z and c reach both local minima a and b , node w_i with $i < k$ ($i > k$) reaches a (b , respectively), and node v_i with $i < t$ ($i > t$) reaches a (b , respectively). These will create a set of triangles such that γ is homotopy equivalent to π , i.e. loop-free. \square

Proof of Theorem 3. The proof is analogous to that of Theorem 2. \square

S-2. CURRENT ON EDGES AND PATHS. TRANSITION PATH THEORY

The energy landscape gives us a global picture for the different attraction basins on the network. To understand the dynamics between the different basins, the transition path theory (TPT) provides a natural tool.

The transition path theory was originally introduced in the context of continuous-time Markov process on continuous state space [27] and discrete state space [28], see [29] for a review. Another description of discrete transition path theory for molecular dynamics can be also found in [30]. Here we adapt the theory to the setting of discrete time Markov chain with transition probability matrix P . We assume reversibility in the following presentation, the extension to non-reversible Markov chain is straightforward.

Given two sets A and B in the state space V , the transition path theory tells how these transitions between the two sets happen (mechanism, rates, etc.). If we view A as a reactant state and B as a product state, then one transition from A to B is a reaction event. The reactive trajectories are those part of the equilibrium trajectory that the system is going from A to B . To make the notion more precise, define the ordered family of times $\{n_j^A, n_j^B\}$ such that

$$\begin{aligned} X_{n_j^A} &\in A, \quad X_{n_j^B} \in B, \\ X_n &\in V \setminus (A \cup B), \quad \forall n, n_j^A < n < n_j^B. \end{aligned}$$

Hence, a reaction happens from time n_j^A to time n_j^B .

Definition 1. Given any equilibrium trajectory $\{X_n\}$, we call each portion of the trajectory of between n_j^A and n_j^B a *AB-reactive trajectory*. We call the time during which the reaction occurs the *reactive times*

$$(S-10) \quad R = \bigcup_{j \in \mathbb{Z}} (n_j^A, n_j^B).$$

The central object in transition path theory is the committor function. Its value at x gives the probability that a trajectory starting from x will hit the set B first than A , *i.e.*, the success rate of the transition at x . Given two sets A and B in the state space, q satisfies the equation

$$(S-11) \quad \begin{cases} \sum_{y \in V} p_{xy} q(y) - q(x) = 0, & x \notin A \cup B; \\ q(x) = 0, & x \in A; \\ q(x) = 1, & x \in B, \end{cases}$$

The committor function provides natural decomposition of the graph. If $q(x)$ is less than 0.5, x is more likely to reach A first than B ; so that $\{x \mid q(x) < 0.5\}$ gives the set of points that are more attached to set A .

Once the committor function is given, the statistical properties of the reaction trajectories between A and B can be quantified. We state several propositions characterizing transition mechanism from A to B . The proof of them is an easy adaptation of [27, 28] and will be omitted.

Proposition 2 (Probability distribution of reactive trajectories). *The probability distribution of reactive trajectories*

$$(S-12) \quad \pi_R(x) = \mathbb{P}(X_n = x, n \in R)$$

is given by

$$(S-13) \quad \pi_R(x) = \pi(x)q(x)(1 - q(x)).$$

The distribution π_R gives the equilibrium probability that a reactive trajectory visits x . It provides information about the proportion of time the reactive trajectories spend in state x along the way from A to B .

Proposition 3 (Reactive current from A to B). *The reactive current from A to B , defined by*

$$(S-14) \quad J(xy) = \mathbb{P}(X_n = x, X_{n+1} = y, \{n, n+1\} \subset R),$$

is given by

$$(S-15) \quad J(xy) = \begin{cases} \pi(x)q(x)P_{xy}(1 - q(y)), & x \neq y; \\ 0, & \text{otherwise.} \end{cases}$$

The reactive current $J(xy)$ gives the average rate the reactive trajectories jump from state x to y . From the reactive current, we may define the effective reactive current on an edge and transition current through a node which characterizes the importance of an edge and a node in the transition from A to B , respectively.

Definition 2. The *effective current* of an edge xy is defined as

$$(S-16) \quad J^+(xy) = \max(J(xy) - J(yx), 0).$$

The *transition current* through a node $x \in V$ is defined as

$$(S-17) \quad T(x) = \begin{cases} \sum_{y \in V} J^+(xy), & x \in A \\ \sum_{x \in V} J^+(xy), & x \in B \\ \sum_{y \in V} J^+(xy) = \sum_{x \in V} J^+(xy), & x \notin A \cup B \end{cases}$$

In applications one often examines partial transition current through a node connecting two communities $V^- = \{x : q(x) < 0.5\}$ and $V^+ = \{x : q(x) \geq 0.5\}$, e.g. $\sum_{y \in V^+} J^+(xy)$ for $x \in V^-$, which shows relative importance of the node in bridging communities.

The reaction rate ν , defined as the number of transitions from A to B happened in a unit time interval, can be obtained from adding up the probability current flowing out of the reactant state. This is stated by the next proposition.

Proposition 4 (Reaction rate). *The reaction rate is given by*

$$(S-18) \quad \nu = \sum_{x \in A, y \in V} J(xy) = \sum_{x \in V, y \in B} J(xy).$$

Finally, the committor functions also give information about the time proportion that an equilibrium trajectory comes from A (the trajectory hits A last rather than B).

Proposition 5. *The proportion of time that the trajectory comes from A (resp. from B) is given by*

$$(S-19) \quad \rho^A = \sum_{x \in V} \pi(x)q(x), \quad \rho^B = \sum_{x \in V} \pi(x)(1 - q(x)).$$

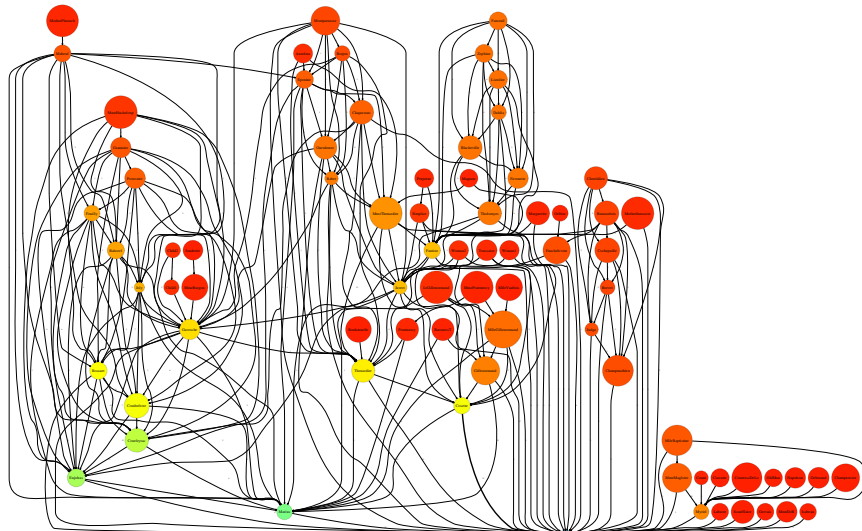


FIGURE S-1. The Les Misérables Network. The whole network has 77 nodes as main characters in Victor Hugo’s novel, Les Misérables, where Valjean is the only local minimum (global minimum) as the novel is written around his experience.

S-3. SUPPLEMENTARY FIGURES

The first figure is the whole co-appearance network of 77 main characters in the novel, Les Misérables, by Victor Hugo [25]. It is an undirected weighted graph with edge weights as the number of co-appearances for a pair of characters. Without thresholding this network contains one local minimum, Valjean. However a thresholding with edge weight greater than 7 gives rise to the subnetwork in the main text.

The second figure contains a list of structural information on 54 metastable states. It contains a typical crystal structure in each state, and some free energy plots on certain reaction coordinates. From these pictures one can read various structural properties of critical nodes in LAO-protein binding transition network discussed in the main text. More information about this system can be found in [26].

The third figure shows the ranking of transition currents out of misbound state 18 over eleven transition pathways. The experiment selects each of the eleven solvated states $\{43, \dots, 53\}$ as the source set and the misbound state 10 as the common target set. In each of the eleven experiments, relative transition current out of state 18 divided by total transition current from the source, is recorded and plotted in a descending order.

REFERENCES

- [1] Watts DJ, Strogatz SH (1998) Collective dynamics of ‘small world’ networks. *Nature* 393:440–442.
- [2] Barabási AL, Albert R (1999) Emergence of scaling in random networks. *Science* 286:509–512.
- [3] Strogatz SH (2001) Exploring complex networks. *Nature* 410:268–276.
- [4] Chung FR, Lu L (2006) *Complex Graphs and Networks* (AMS-CBMS).



FIGURE S-2. (Courtesy by Xuhui Huang) Three types of pictures for each of the 54 metastable states: on the left is the crystal structure of a representative conformation in each state, on the right are free energy plots of the protein opening angle versus twisting angle (O, T) (red), as well as the distance between the ligand and the binding site versus the opening angle (L,O) (blue). The green and blue crosses correspond to X-ray structures of the bound (PDB ID: 1LAF) and apo (PDB ID: 2LAO) conformations respectively.

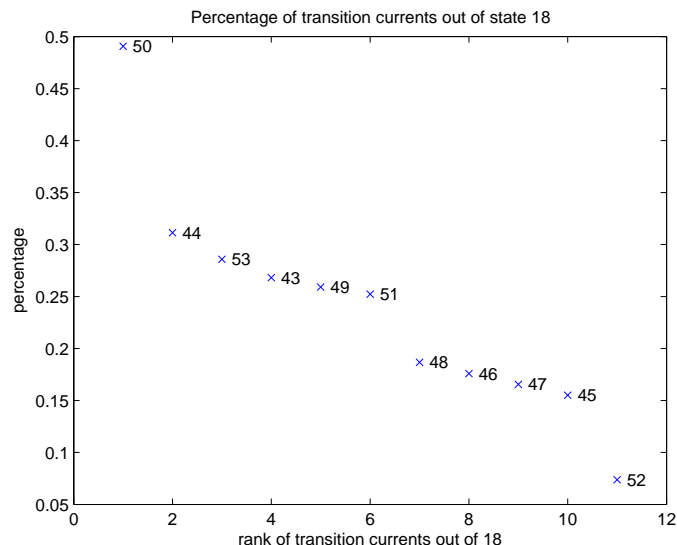


FIGURE S-3. Transition Currents out of misbound state 18, with source set from each of solvated states $\{43, \dots, 53\}$ and target set as bound state 10.

- [5] Tenenbaum J, de Silva V, Langford J (2000) A global geometric framework for nonlinear dimensionality reduction. *Science* 290:2323–2326.
- [6] Roweis ST, Lawrence SK (2000) Locally linear embedding. *Science* 290:2319–2323.
- [7] Seung HS, Lee DD (2000) The manifold ways of perception. *Science* 290:2268–2269.
- [8] Belkin M, Niyogi P (2003) Laplacian eigenmaps for dimensionality reduction and data representation. *Neural Computation* 15:1373–1396.
- [9] Donoho DL, Grimes C (2003) Hessian eigenmaps: Locally linear embedding techniques for high-dimensional data. *Proceedings of the National Academy of Sciences of the United States of America* 100:5591–5596.
- [10] Coifman RR, et al. (2005) Geometric diffusions as a tool for harmonic analysis and structure definition of data: Diffusion maps i. *Proceedings of the National Academy of Sciences of the United States of America* 102:7426–7431.
- [11] Edelsbrunner H, Letscher D, Zomorodian A (2002) Topological persistence and simplification. *Discrete and Computational Geometry* 28:511–533.
- [12] Ghrist R (2007) Barcodes: the persistent topology of data. *Bulletin of the American Mathematical Society* 45:61–75.
- [13] Edelsbrunner H, Harer J (2008) Persistent homology: a survey. *Contemporary Mathematics* pp 1–26.
- [14] Carlsson G (2009) Topology and data. *Bulletin of the American Mathematical Society* 46:255–308.
- [15] Wales DJ (2003) Energy Landscapes. Cambridge University Press.
- [16] Toroczkai Z, Bassler KE (2004) Jamming is limited in scale-free systems. *Nature* 428:55455.
- [17] Toroczkai Z, Kozma B, Bassler KE, Hengartner NW, Korniss G (2008) Gradient networks. *Journal of Physics A: Mathematical and Theoretical* 41:155103.
- [18] Yang B., Liu JM, Feng JF (2012) On the spectral characterization and scalable mining of network communities. *IEEE Transactions on Knowledge and Data Engineering* 24:326–337.
- [19] Milnor J (1963) *Morse Theory* (Princeton University Press).
- [20] Edelsbrunner H, Harer J, Zomorodian A (2003) Hierarchical morse-smale complexes for piecewise linear 2-manifolds. *Discrete and Computational Geometry* 30:87–107.
- [21] Forman R (1998) Morse theory for cell complexes. *Advances in Mathematics* 134:90–145.

- [22] Knill O (2012) A Graph Theoretical Poincare-Hopf Theorem. *arXiv:1201.1162v1*, 2012.
- [23] Zachary WW (1977) An information flow model for conflict and fission in small groups. *Journal of Anthropological Research* 33:452–473.
- [24] Milosavljevic N, Morozov D, Skraba P (2011) Zigzag persistent homology in matrix multiplication time. *Proceedings of the 27th Annual Symposium on Computational Geometry (SoCG'11)* pp 216–225.
- [25] Knuth DE (1993) *The Stanford GraphBase: A Platform for Combinatorial Computing* (Addison-Wesley).
- [26] Silva DA, Bowman GR, Sosa-Peinado A, Huang X (2011) A role for both conformational selection and induced fit in ligand binding by the lao protein. *PLoS Computational Biology* 7:e1002054.
- [27] E W, Vanden-Eijnden E (2006) Towards a theory of transition paths. *J. Stat. Phys.* 123:503–523.
- [28] Metzner P, Schütte C, Vanden-Eijnden E (2009) Transition path theory for markov jump processes. *Multiscale Model. Simul.* 7:1192.
- [29] E W, Vanden-Eijnden E (2010) Transition-path theory and path-finding algorithms for the study of rare events. *Annual Review of Physical Chemistry* 61:391–420.
- [30] Noè F, Schütte C, Vanden-Eijnden E, Reich L, Weigl TR (2009) Constructing the equilibrium ensemble of folding pathways from short off-equilibrium simulations. *Proceedings of the National Academy of Sciences of the United States of America* 106:19011–19016.

WEINAN E, BEIJING INTERNATIONAL CENTER FOR MATHEMATICAL RESEARCH, PEKING UNIVERSITY, BEIJING 100871, P.R. CHINA; DEPARTMENT OF MATHEMATICS AND PROGRAM IN APPLIED AND COMPUTATIONAL MATHEMATICS, PRINCETON UNIVERSITY, PRINCETON, NJ 08544-1000 U.S.A.

E-mail address: weinan@math.princeton.edu

JIANFENG LU, COURANT INSTITUTE OF MATHEMATICAL SCIENCES, NEW YORK UNIVERSITY, 251 MERCER ST., NEW YORK, NY, 10012-1185, U.S.A.

E-mail address: jianfeng@cims.nyu.edu

YUAN YAO, SCHOOL OF MATHEMATICAL SCIENCES, LMAM AND LMP, PEKING UNIVERSITY, BEIJING 100871, P.R. CHINA

E-mail address: yuany@math.pku.edu.cn